Young S. Shin
Jae-Jin Jeon
Department of Mechanical Engineering
Naval Postgraduate School
Monterey, CA 93943

Pseudo Wigner–Ville Time-Frequency Distribution and Its Application to Machinery Condition Monitoring

Machinery operating in a nonstationary mode generates a signature that at each instant of time has a distinct frequency. A Time-frequency domain representation is needed to characterize such a signature. Pseudo Wigner–Ville distribution is ideally suited for portraying a nonstationary signal in the time–frequency domain and is carried out by adapting the fast Fourier transform algorithm. The important parameters affecting the pseudo Wigner–Ville distribution are discussed and sensitivity analyses are also performed. Practical examples of an actual transient signal are used to illustrate its dynamic features jointly in time and frequency. © *1993 John Wiley & Sons, Inc.**

INTRODUCTION

The physical condition or state of health of machineries that operate in transient or other nonstationary modes are difficult to predict with any degree of accuracy. It is common to practice periodic preventive maintenance on these machineries in order to avoid failures and prolong the useful operating life of the equipment.

In order to assess the physical condition of machinery without complete disassembly, a physical measurement of its vibrations is conducted using an accelerometer. Other sensors, such as temperature or pressure transducers, could also be used. There are other methods, including motor current signature analysis on electrically driven machinery and wear debris analysis that could be used. However, vibrations are used predominantly for machinery condition monitoring. The vibrations are recorded in the time domain.

There is a need for a method to represent the time dependent events that occur with machinery operating in nonstationary modes. At each instant in time as the speed of the machinery changes, the frequency content will also change. The pseudo Wigner–Ville distribution (PWVD) is the method chosen to portray these time-dependent changes. This is a continuation of work initially performed and published by Rossano, Hamilton, and Shin [1990].

The PWVD is a three dimensional (time, frequency, amplitude) representation of an input signal and is ideally suited for describing transient or other nonstationary phenomena. The Wigner distribution (WDF) has been used in the areas of optics [Bastiaans, 1978, 1979; Bartelt, Brenner, and Lohmann, 1990] and speech analysis [Riley, 1989; Veley and Absher, 1989]. Wahl

Shock and Vibration, Vol. 1, No. 1, pp. 65–76 (1993)

CCC 1070-9622/93/01065-12

and Bolton [1990] used it to identify structure-borne noise components. Flandrin, Garreau, and Puyal [1989] recently proposed its use in the area of machinery condition monitoring and diagnostics; Forrester [1990] is investigating its use in gear fault detection.

For such a nonstationary signal analysis, a spectrogram is commonly used that is based on the assumption that it is a collection of short duration stationary signals. A major drawback of this approach is that the frequency resolution is directly affected by the duration of short stationary time, which subsequently determines the time resolution. A method for time–frequency domain signal characterization that overcomes this drawback is the WDF [Wigner, 1932] first introduced by Wigner in 1932 to study the problem of statistical equilibrium in quantum mechanics. The frequency and time resolutions of the WDF are not determined by the short duration but rather determined by the selection of desired resolution of the signal itself.

This article discusses the important parameters affecting the PWVD in order to monitor machinery condition and presents numerical examples of PWVD using synthetically generated signals. It is found that the PWVD is very effective in monitoring machinery condition that operates in nonstationary modes.

PSEUDO WIGNER–VILLE DISTRIBUTION

Signals associated with most vibrational phenomena are, in general, time varying, which means that their characteristics change with time and they have various features in different time frames. The general spectrogram usually requires a large time–bandwidth product to reduce the estimated bias and variability. In the case of a signal containing some transients or nonstationary conditions, the traditional approach in signal analysis fails to describe the dynamics of the signal's frequency component changes.

The general expression of the time-frequency distribution of a signal, $w(t, \omega)$ is given by, [Cohen, 1989]

$$w(t, \omega) = \frac{1}{2\pi} \int \int \int e^{-j\theta t - j\tau\omega - j\theta u} \phi(\theta, \tau) \, s^* \left(u - \frac{\tau}{2}\right) s \left(u + \frac{\tau}{2}\right) du \, d\tau \, d\theta \tag{1}$$

where $s(u)$ is the time signal, $s^*(u)$ is its complex conjugate, and $\phi(\theta, \tau)$ is an arbitrary function called the kernel. By choosing different kernels, different distributions are obtained. Wigner distribution is obtained by taking $\phi(\theta, \tau) = 1$. The range of all integrations is from $-\infty$ to ∞ unless otherwise noted.

Substituting the kernel $\phi(\theta, \tau) = 1$ in Eq. (1), the WDF is obtained,

$$w(t, \omega) = \int s^* \left(t - \frac{\tau}{2}\right) s \left(t + \frac{\tau}{2}\right) e^{-j\tau\omega} \, d\tau. \tag{2}$$

One of the basic frequency representations of a signal is the power density spectrum, which characterizes the signal's frequency component distribution. The power spectral density function $p(\omega)$ of a signal $s(t)$ can be related to the Fourier transform of the signal's autocorrelation function $R(\tau)$:

$$p(\omega) = \int e^{-j\omega\tau} R(\tau) \, d\tau \tag{3}$$

with

$$R(\tau) = \int s(t) \, s(t + \tau) \, dt. \tag{4}$$

From this relation a time-dependent power spectral density function can be written as

$$w(t, \omega) = \int R_t(\tau) \, e^{-j\omega\tau} \, d\tau \tag{5}$$

where now $R_t(\tau)$ is a time-dependent or local autocorrelation function. Mark [1970] argued for symmetry,

$$R_t(\tau) = s^* \left(t - \frac{\tau}{2}\right) s \left(t + \frac{\tau}{2}\right), \tag{6}$$

which gives the WDF.

The properties of the WDF [Claasen and Mecklenbrauker, 1980; Yen, 1987] are summarized and reinterpreted with this new formulation as follows: (i) the WDF is a real-valued function; (ii) the integral of the WDF with respect to frequency and time yields the instantaneous signal power and the signal's power spectral density respectively; (iii) a time or frequency shift in the signal has the same shift in the WDF; (iv) the WDF is symmetrical in time for a given signal; (v) the WDF is not always positive; (vi) the integration of the square of the WDF equals the square of the time integration of the signal's power.

IMPLEMENTATION WITH DIGITAL SIGNAL PROCESSING

There are two distinct advantages for the calculation of the WDF. First, it has the form of the Fourier transform (FFT) and the existing FFT algorithm can be adapted for its computation. Second, for a finite time signal, its integration is finite within the record length of the existing signal.

The discrete time Wigner distribution as developed by Claasen and Mecklenbrauker [1980] is expressed by,

$$w(t, \omega) = 2 \sum_{\tau=-\infty}^{\tau=\infty} e^{-j2\omega\tau} s(t + \tau)\, s^*(t - \tau). \quad (7)$$

The discrete version of Eq. (7) for a sampled signal $s(n)$, where $n = 0$ to $N - 1$, has the form,

$$w(l, k) = \frac{1}{N} \sum_{n=0}^{N-1} s(l + n)\, s^*(l - n)\, e^{-j(4\pi/N)nk}, \quad k = 0, 1, 2, \ldots N - 1 \quad (8)$$

where $s(m) = 0$ for $m < 0$ and $m > N - 1$. However, in order to utilize the FFT algorithm, it must be assumed that the local autocorrelation function has a periodicity of N. This is just for operational convenience and should not apply to the interpretation of $s(m)$. Eq. (8) can be rewritten as,

$$\begin{aligned} & w[l, k + m(N/2)] \\ &= \frac{1}{N} \sum_{n=0}^{N-1} s(l + n)\, s^*(l - n)\, e^{-j(4\pi/N)n[k+m(N/2)]} \\ &= \frac{1}{N} \sum_{n=0}^{N-1} s(l + n)\, s^*(l - n)\, e^{-j(4\pi/N)nk} e^{-jmn2\pi} \\ &= w(l, k) \end{aligned} \quad (9)$$

because $e^{-jmn2\pi} = 1$ for m = integers.

Eq. (9) indicates that the WDF has a periodicity of $N/2$. Hence, even when the sampling of $s(t)$ satisfies the Nyquist criteria, there are still aliasing components in the WDF. A simple approach to avoid aliasing is to use an analytic signal before computing the WDF. Ville [1948] proposed the use of the analytic signal in time–frequency representations of a real signal. An analytic signal is a complex signal that contains both real and imaginary components. The imaginary part is obtained by Hilbert transform. The analytic signal may be expressed by,

$$s(t) = s_r(t) + jH\{s_r(t)\} \quad (10)$$

where $H\{s_r(t)\}$ is a Hilbert transform and generated by the convolution of the impulse response $h(t)$ of a 90-degree phase shift as follows:

$$\begin{aligned} H\{s_r(t)\} &= s_r(t) * h(t) \\ h(t) &= \frac{2 \sin^2(\pi t/2)}{\pi t}, \quad t \neq 0, \\ &= 0, \quad t = 0, \end{aligned} \quad (11)$$

where * denotes the convolution. Rewriting Eq. (11) to discrete form,

$$H\{s_r(n)\} = \sum_{m=-\infty}^{\infty} h(n - m)\, s_r(m). \quad (12)$$

The distribution resulting from an analytic signal being processed through the WDF is commonly termed as Wigner-Ville distribution.

To calculate the WDF of the sampled data, it is necessary that Eq. (8) be modified to Eq. (13), because the WDF has $N/2$ periodicity.

$$w(m\Delta t, k\Delta\omega) = 2\Delta t \sum_{n=0}^{2N-1} s[(m + n)\Delta t]\, s^*[(m - n)\Delta t]\, e^{-j2\pi nk/(2N)} \quad (13)$$

where $\Delta\omega = \pi/(2N\Delta t)$ and Δt is the sampling interval. The algorithm used in this paper is based on one written by Wahl and Bolton [1990] and can be expressed as:

$$\begin{aligned} w(m\Delta t, k\Delta\omega) &= \mathrm{RE}\{2\Delta t\ \mathrm{FFT}[\mathrm{corr}(i)]\} \\ \mathrm{corr}(i) &= s(m + i - 1)\, s^*(m - i + 1), \quad m \geq i \\ &= 0, \quad m < i \end{aligned} \quad (14)$$

where

$$1 \leq i \leq N + 1,$$

$$\mathrm{corr}(2N - i + 2) = \mathrm{corr}^*(i), \quad 2 \leq i \leq N$$

The frequency resolution, $\Delta\omega$, in Eq. (13) is different from that obtained by FFT of the original N point time record in two respects. The first difference is that the argument of the time signal and its conjugate contains a factor of 1/2, and

secondly, the autocorrelation of the time signal is twice the length of the original record and therefore the FFT is evaluated over $2N$ points. The result is that the WDF frequency resolution is one-fourth the resolution of an ordinary power spectrum density function.

Before processing the WDF, a modified Hamming window is applied to the time domain signal to reduce the leakage caused by the discontinuity of the finite record of data, which will be called as data tapering. This type of window is preferable because it alters the amplitude of fewer data points at the beginning and the end of the data block. A modified Hamming window, $D(t)$ is given by:

$$D(t) = \begin{cases} 0.54 - 0.46 * \cos[10\pi t/T), & 0 \le t \le T/10, \\ 1.0, & T/10 \le t \le 9T/10, \\ 0.54 - 0.46 * \cos[10\pi(T - t)/T], & 9T/10 \le t \le T. \end{cases} \tag{15}$$

Two other characteristics of the WDF should be also noted. First, the WDF of the sum of two signals is equal to the sum of the WDF of each signal plus the cross-terms that appear when the cross-correlation of the two signals is nonzero. Second, the WDF may have negative values that may be largely caused by interference due to the presence of these cross-terms. In the case of input signals that contain multifrequency components, the Wigner–Ville distribution of most signals are very complicated and difficult to interpret.

There are two methods to suppress the interference components of the WDF. Claasen and Mecklenbrauker [1980] describe the application of a sliding window in the time domain before calculating WDF. The WDF obtained with a window function is called the pseudo–WDF. A second option is to smooth the WDF with a sliding averaging window in the time–frequency plane. In both cases the result is to deemphasize components arising from calculations and to emphasize deterministic components. Obviously, averaging a Wigner–Ville distribution will result in a PWVD.

In this research, a sliding exponential window in the time–frequency domain was chosen. That is, a Gaussian window function, $G(t, \omega)$ is selected to reduce the interference and to avoid the negative values as follows: let

$$G(t, \omega) = \frac{1}{2\pi\sigma_t\sigma_\omega} e^{-[(t^2/2\sigma_t^2)+(\omega^2/2\sigma_\omega^2)]}, \tag{16}$$

then

$$w(t, \omega) = \frac{1}{2\pi} \int\int w(t', \omega') \, G(t - t', \omega - \omega') \, dt' \, d\omega' > 0 \tag{17}$$

where σ_t, $\sigma_\omega > 0$ and $\sigma_t\sigma_\omega \ge 1/2$ [Cartwright, 1976]. The time and frequency resolution's Δt and $\Delta\omega$ of this Gaussian window are related by,

$$\sigma_t = j\Delta t, \quad \sigma_\omega = k\Delta\omega \tag{18}$$

in the discrete form. Then the condition for the WDF to be positive in this case is

$$j\Delta t k\Delta\omega > 1/2. \tag{19}$$

This is the time–frequency version of Heisenberg's uncertainty relation [Yen, 1987]. If the segmentation of time and frequency for a given signal from Eq. (2) violates this uncertainty principle, the corresponding WDF may not be positive.

To perform the convolution on the sampled WDF, the Gaussian window function was applied to the range $\pm 2\sigma_t$ and $\pm 2\sigma_\omega$. Selecting ω and t to be the multiple of time and frequency steps, the sampled Gaussian window function is expressed by,

$$G(p, q) = \frac{1}{2\pi jk\Delta t \, \Delta\omega} e^{-[(p^2/2j^2)+(q^2/2k^2)]} \tag{20}$$

where p and q are integer numbers in the range $\pm 2j$ and $\pm 2k$, respectively. The convolution of the sampled WDF and the Gaussian window function can be evaluated as follows:

$$w'(l, m) = \frac{\Delta t\Delta\omega}{2\pi} \sum_{p=l-j}^{l+j} \sum_{q=m-k}^{m+k} w(p, q) \, G(p - l, q - m) \tag{21}$$

where $w'(l, m)$ is the smoothed WDF or PWVD.

Figure 1 shows a block diagram for computational sequence of the PWVD. A time-varying

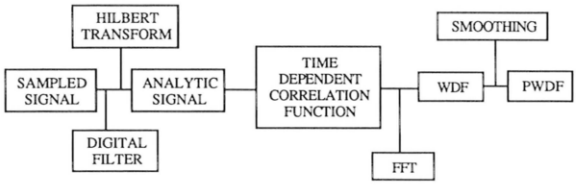

FIGURE 1 Computational block diagram of pseudo Wigner–Ville distribution.

signal sampled with the Nyquist rate is first high passed through a digital filter if the signal involves the zero frequency component, the DC component, and converted into the analytic signal through a Hilbert transform. Then, the time-dependent correlation function is computed and the result is the WDF in terms of both time and frequency domain by FFT. The final step is to compute the convolution with a Gaussian window.

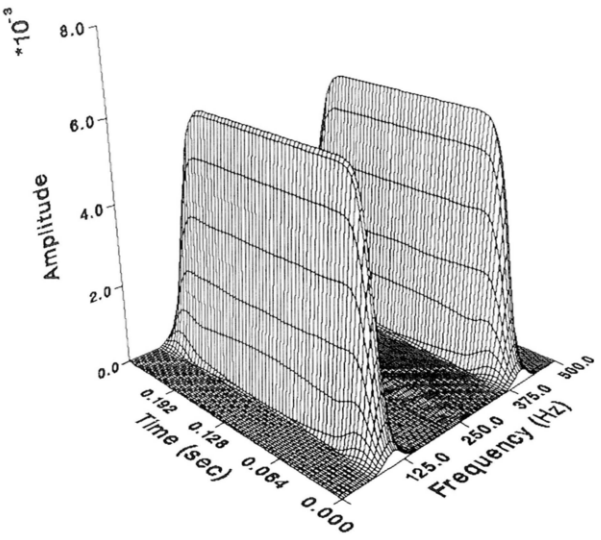

FIGURE 2 Pseudo Wigner–Ville distribution of 100 and 400 Hz pure sine waves. f_s = 1000 Hz, N = 256, and smoothing window size = 10 × 10.

EXAMPLES AND DISCUSSIONS

Machinery operating in a transient mode generates a signature in which the frequency content varies at each instant of time. To characterize such signatures and to understand the vibrational behavior of such machineries, time–frequency domain representation of the signal is needed. As discussed in the previous sections, Wigner distribution is a signal transformation that is particularly suited for the time–frequency analysis of nonstationary signals. There are many advantages of using PWVD for both steady and transient signals. However, there are also several disadvantages, for example, the drastic increase of peak value when the frequency content of signal changes abruptly. A computer program has been developed for PWVD and is continuously updated [Jeon and Shin, in prep.]. Two different versions are available at the present time: workstation and IBM PC compatible.

Harmonic Wave

Figure 2 shows the PWVD of the pure sine wave with two frequency components (100 Hz, 400 Hz), respectively. The modified Hamming window was applied to the time-domain signal and the Gaussian smoothing window function was applied on time–frequency domain Wigner–Ville distribution. The slope of the end edges are due to data tapering by using the modified Hamming window. Figure 3 shows the PWVD of the sine wave that have the 10% and 50% signal-to-noise ratio, respectively. The shape of PWVD is changed at the crest by the contamination of noise. The crest has the complicated shape with decreasing of signal-to-noise ratio. However, the PWVD represents the signal components from the given signal with noise. The notation f_s and N used in the figures are sampling frequency and the total number of time data points.

Harmonic Wave with Stepwise Frequency Changes

Figure 4 shows (a) the sine wave with stepwise frequency changes, 100, 250, and 500 Hz, and (b) its PWVD. The PWVD shows the time delay and frequency component of the signal. The wide spread of PWVD at the edge of each frequency region is noticed. This phenomenon is caused by the discontinuity of the signal in time domain and the leakage in digital signal processing. This effect may be reduced by applying the data tapering to the actual signal block. Nevertheless the PWVD represented the characteristics of the signal well. PWVD can portray the characteristics of the steady-state signals involving time delay and multifrequency components. If different sizes of the smoothing window are applied, the PWVD amplitude changes, but the total energy remains unchanged.

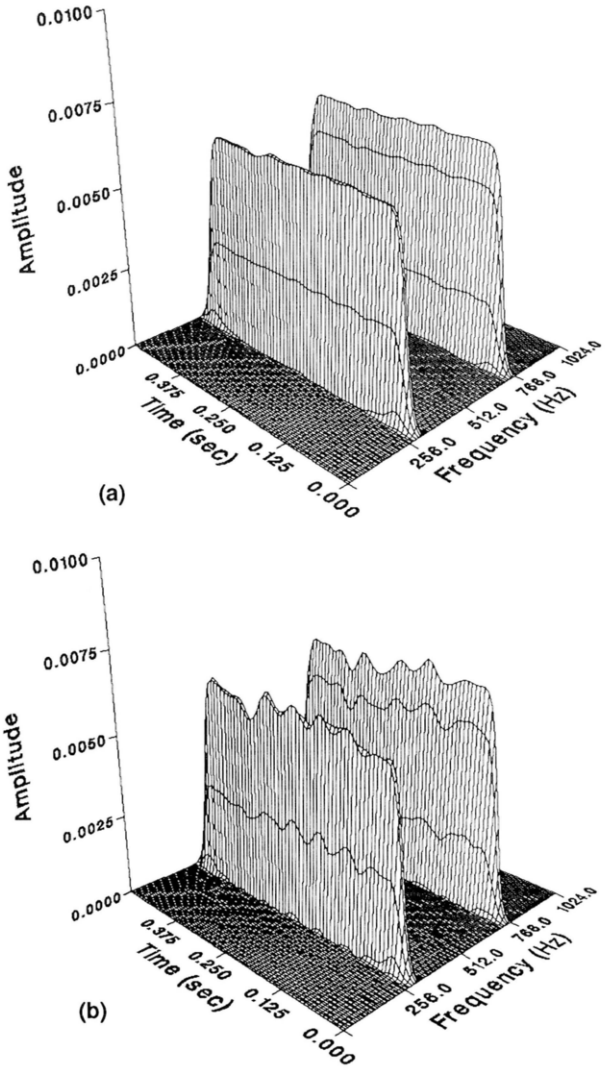

FIGURE 3 Pseudo Wigner–Ville distribution of 300 and 750 Hz sine waves; signal to noise ratio (a) 10% and (b) 50%. f_s = 2048 Hz, N = 1024, and smoothing window size = 18 × 18.

Composite Signal with Two Frequency Components at Each Time

The PWVDs of the nonstationary signals were studied and the results are shown in Figs. 5–8. Figure 5 shows (a) the time signal composed of two sweeping frequency components at each time, one increasing and the other decreasing with the same rate, and (b) its Wigner–Ville distribution (before applying the smoothing window), and (c) its PWVD (after applying the smoothing window), respectively.

The effect of cross (or interference) term is significant and appeared in the average frequency region. This is one of the disadvantages of using the Wigner–Ville distribution but it is a characteristic of the distribution. When a Gaussian window was applied to the Wigner–Ville distribution, the effect of cross-term disappeared. The main lobe of PWVD is wider and its amplitude is significantly reduced. The large peak at the intersection point of two sweeping frequency signals is mainly caused by the doubling effect of amplitudes of two signals.

Linear Chirp Signal

Another type of a nonstationary signal that sweeps up and down in frequency is called a linear chirp signal and is shown in Fig. 6(a). This signal has only one frequency component at each time. The effect of cross-terms appears in the Wigner–Ville distribution, as shown in Fig. 5(b).

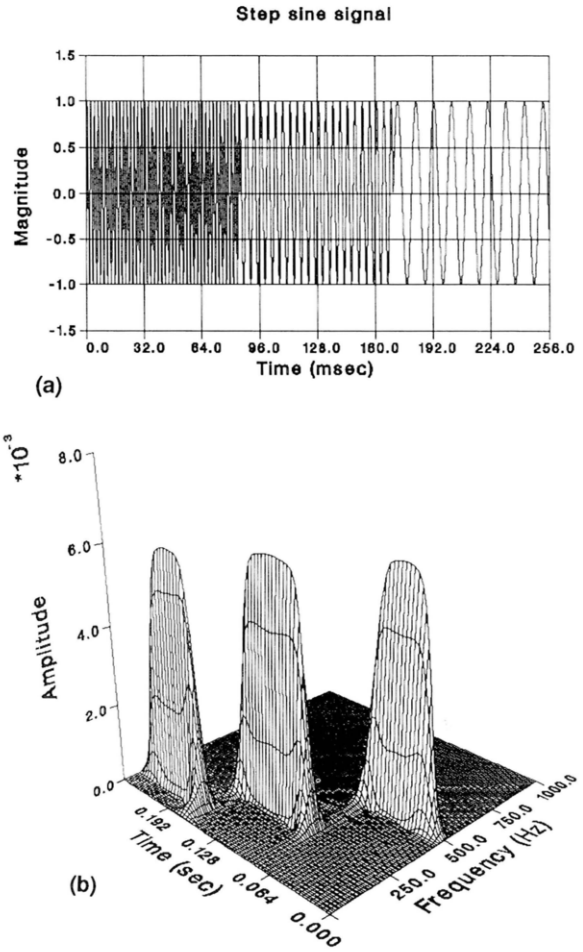

FIGURE 4 Sine wave with stepwise frequency changes: 100, 250, and 500 Hz. f_s = 2000 Hz, N = 512, and smoothing windows size = 10 × 10.

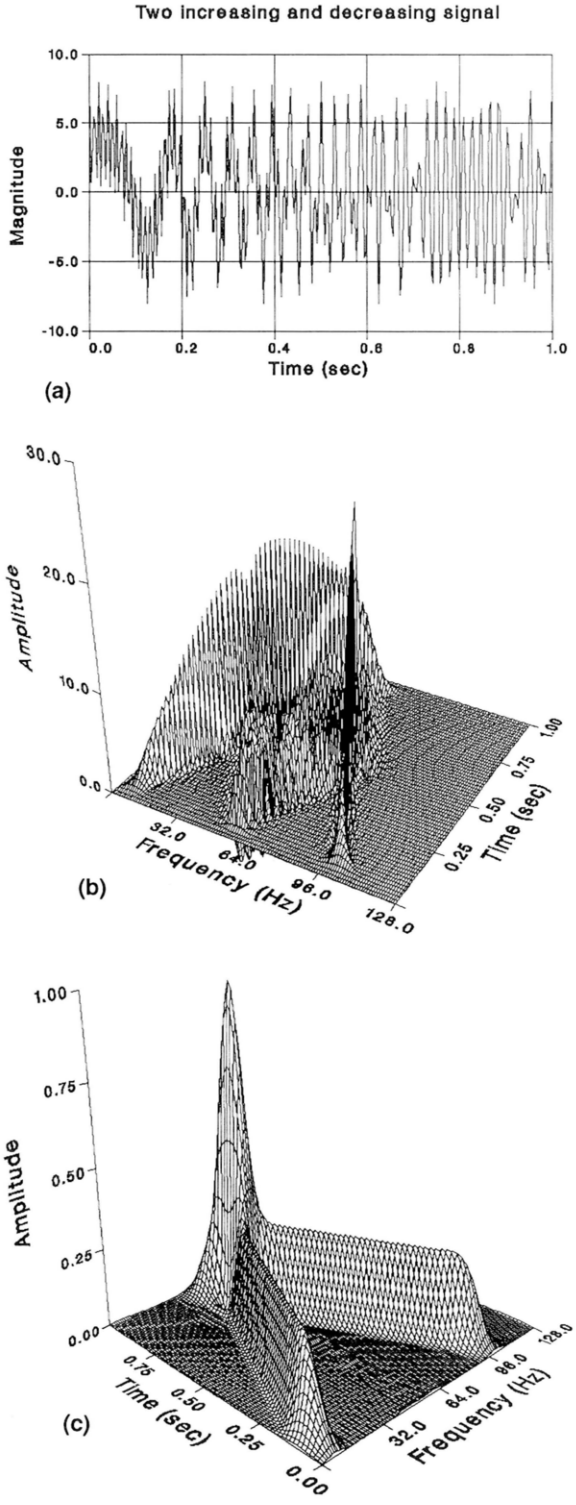

FIGURE 5 Composite signal with two frequency components at each time. (a) Time signal, (b) WDF, and (c) PWVD. $f_s = 256$ Hz, $N = 256$, and smoothing window size = 10×10.

$$s(t) = 4\cos(2\pi 32t^2) + 4\cos\{2\pi[40 + 32(2 - t)]t\}$$

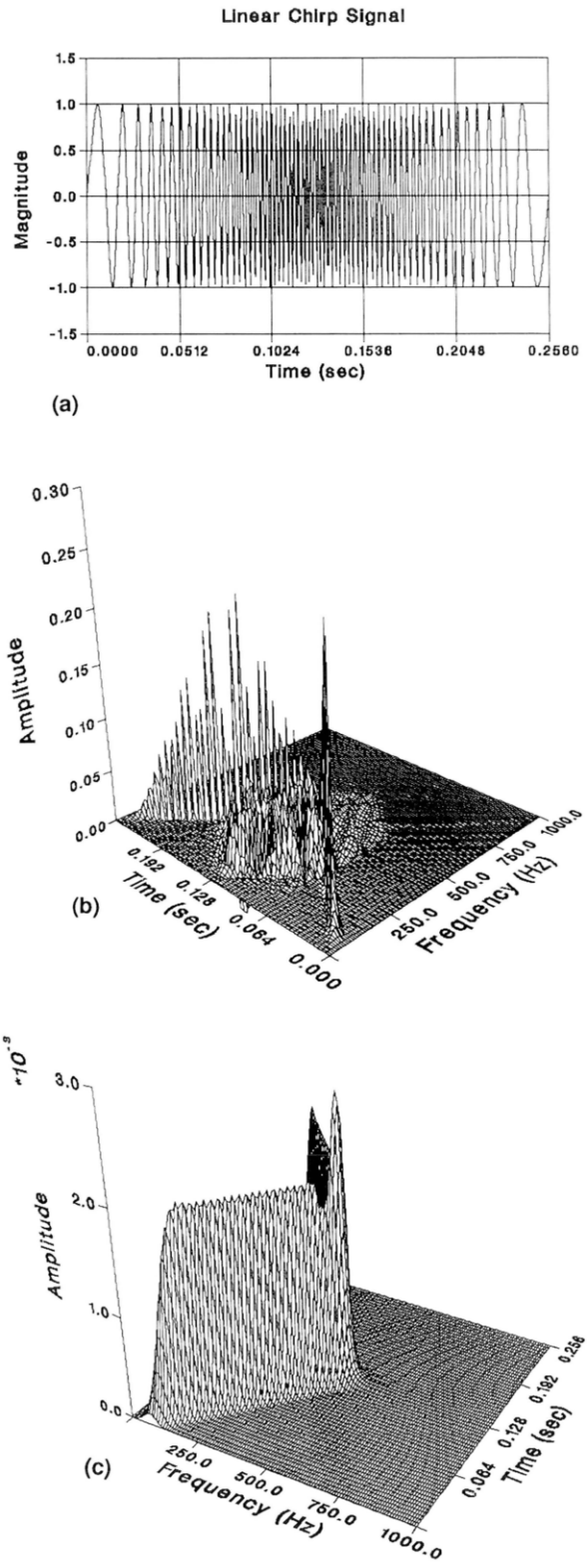

FIGURE 6 Linear chirp signal with one frequency component at each time. (a) Time signal, (b) WDF, and (c) PWVD $f_s = 2000$ Hz, $N = 512$, and smoothing window size = 16×16.

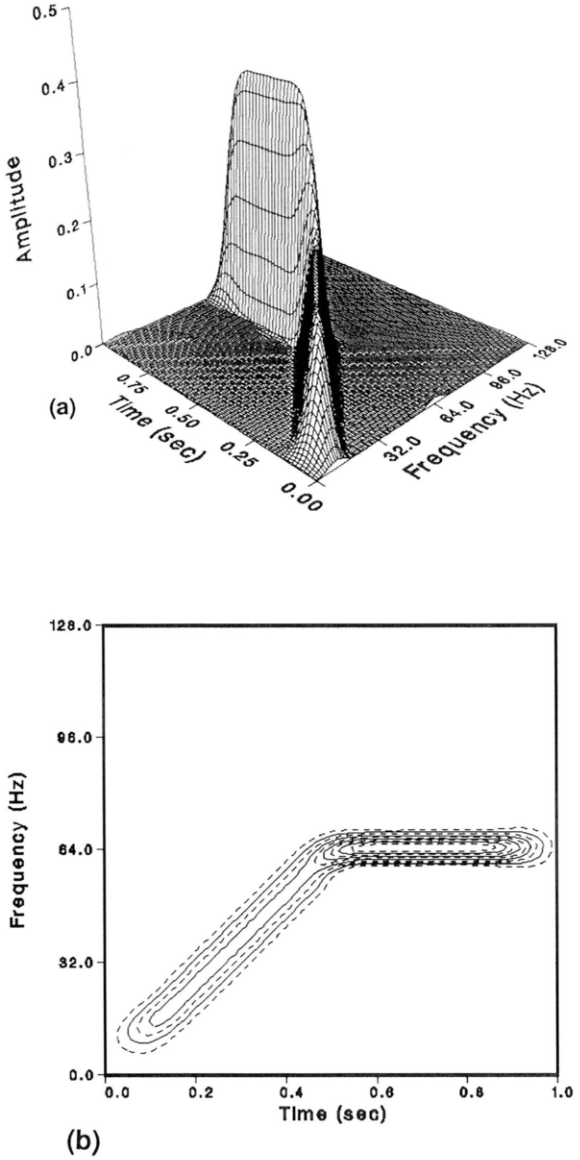

FIGURE 7 PWVD of a composite signal of sweeping-up and steady frequency, (a) PWVD and (b) contour plot f_s = 256 Hz, N = 256, and smoothing windows size = 10 × 10.

The smoothing window was applied to the Wigner–Ville distribution and the result is shown in Fig. 6(c). As expected, the effect of cross-term is significantly reduced. However, the unusual peak (called ghost peak) appeared at the point where the direction of sweep changes. To understand the cause of this phenomenon, the PWVD was integrated along the frequency axis and it was found that the square root of the resultant amplitude was the amplitude of original time sig-

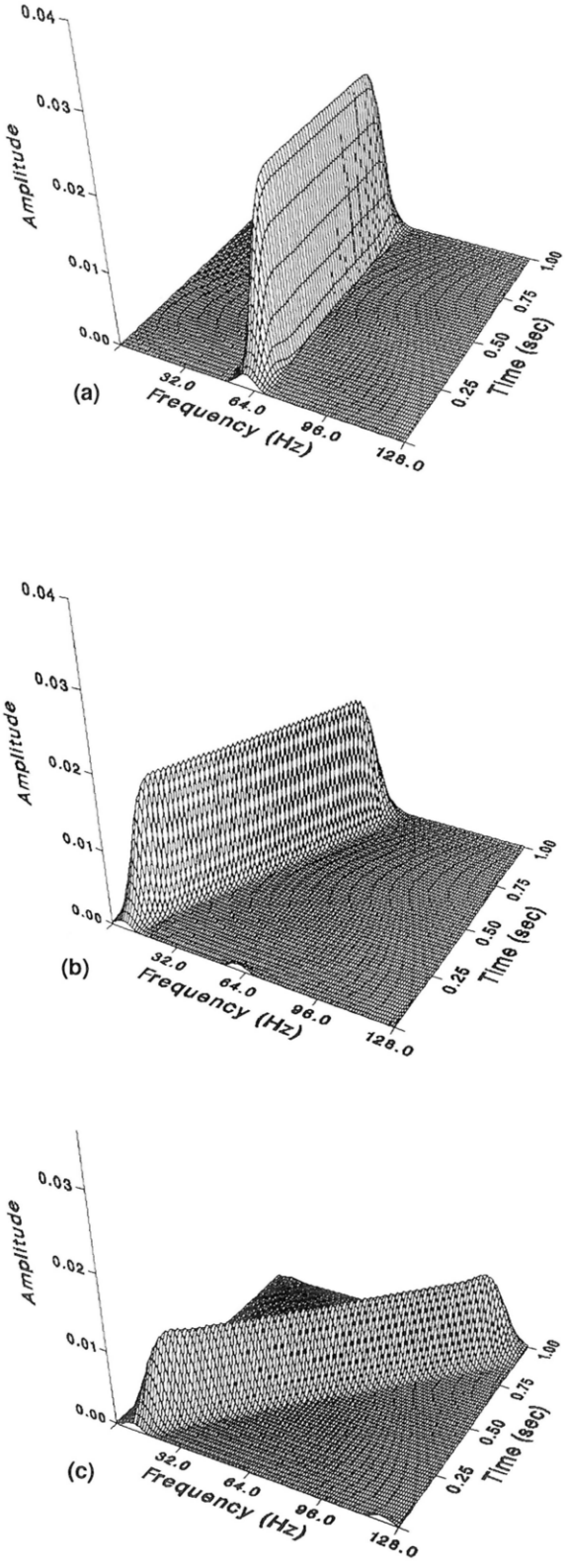

FIGURE 8 The effect of sweep rates to pseudo Wigner–Ville distribution. f_s = 256 Hz, N = 256, and smoothing window size = 10 × 10.

nal, implying that the energy content remained constant. The following function was used to generate the linear chirp signal:

$$s(t) = \sin\left[2\pi\left(30 + \frac{220(i-1)}{256}\right)t\right], \quad 1 \le i \le 256$$

$$s(t) = \sin\left[2\pi\left(30 + \frac{220(512-i)}{256}\right)(0.256\,t)\right], \quad 256 \le i \le 512 \quad (22)$$

where $t = (i - 1)\,dt$ and $dt = 0.0005$.

Composite Signal of Sweeping-Up and Steady Frequency

The signal that sweeps up along the frequency for the first 0.5 second and holds to a constant frequency for the next 0.5 second was considered. This signal is a typical speed profile of the start-up stage of a pump. Figure 7 shows (a) PWVD and (b) its contour plot. The interesting phenomenon was observed in PWVD that the sweep-up portion of the signal (first half second) has a lower amplitude and wider main lobe compared with the steady frequency region of the signal (second half second). When the PWVD was integrated along the frequency axis, it was found that the resultant amplitudes in these two regions are the same. The following functions were used to generate the desired signal:

$$\begin{aligned} s(t) &= 4\cos(2\pi 32t^2), \quad 0 \le t \le 0.5 \text{ second} \\ s(t) &= 4\cos(2\pi 64t), \quad 0.5 \le t \le 1.0 \text{ second} \end{aligned} \quad (23)$$

Sweep Rate Effect

The effect of sweep rate on PWVD was investigated. The sweep rate is the frequency change per unit time. Figure 8 shows the PWVDs of the linear chirp signal with a various sweep rates: (a) has zero sweep rate and (b) has lower sweep rate than (c). It can be seen that the amplitude of PWVD decreases with increasing sweep rate but energy remains unchanged. This result appeared to be caused by Heisenberg's uncertainty relation between time and frequency. However, based on this study, it is clear that the ghost peak (see Fig. 6) appears to be due to the instantaneous zero sweep rate at the point where the direction of sweep changes. Also the peak value is affected by the size of the smoothing window.

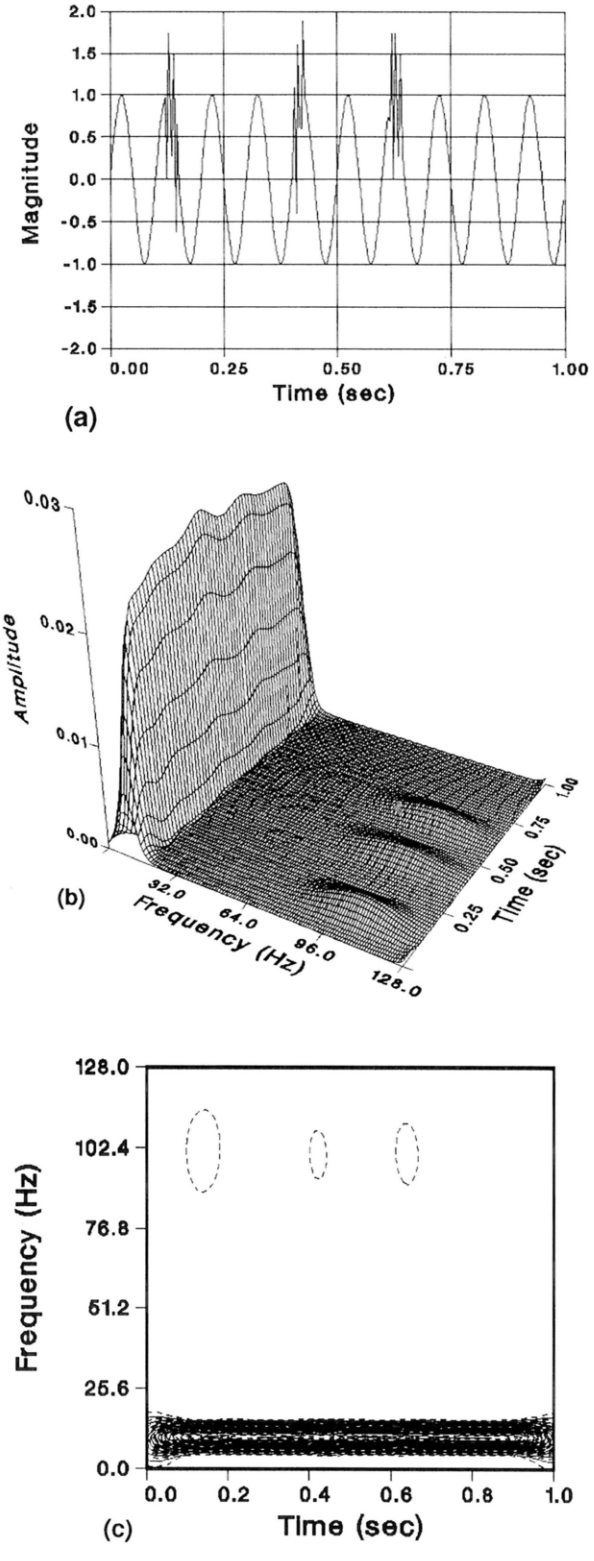

FIGURE 9 Pseudo Wigner–Ville distribution of the signal with glitches. (a) Time signal, (b) PWVD, and (c) the contour plot of the PWVD. f_s = 256 Hz, N = 256, smoothing window size = 10 × 10.

Harmonic Wave with Some Glitches

The interesting phenomena on the signal with an abnormal component as a fault were investigated. Figure 9 shows the PWVD of the harmonic wave with a glitch at a small region of the time record: (a) is the time signal, (b) is the PWVD, and (c) is the contour plot of the PWVD. It can be seen that the PWVD of the signal in Fig. 9(a) well represents the location of each glitch and its frequency components. This characteristic of the PWVD is useful to detect the faults or glitch and to monitor the condition on the vibrational machinery having the periodicity such as a gear train. The general rotating machinery has a periodic signal pattern in the time domain.

Actual Fan Signal

The acceleration signal of a fan was measured at the steady-state speed and the result is shown in Fig. 10. The crest has the complicated shape on the time axis as shown in Fig. 3. The first peak is the fundamental frequency of the blade rate and the second peak is the third harmonics. The third peak is the fundamental frequency of metor by the pole. The measured vibration signal was contaminated with the noise. If the measured signal involves the faults, the PWVD will represent the different pattern having the abnormal frequency components in comparison with the normal condition with time.

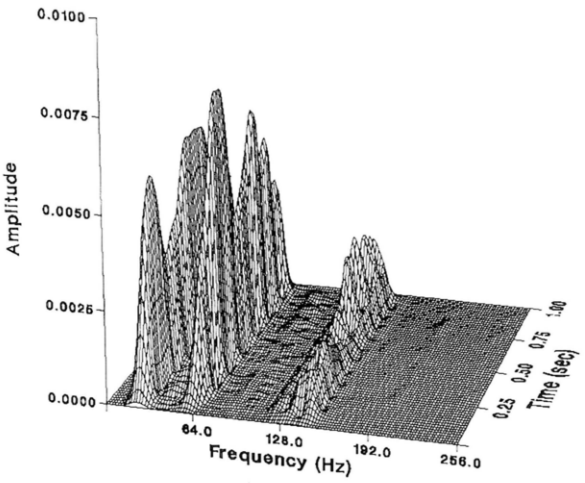

FIGURE 10 Pseudo Wigner–Ville distribution of the actual fan. f_s = 512 Hz, N = 512, smoothing window size = 13 × 13.

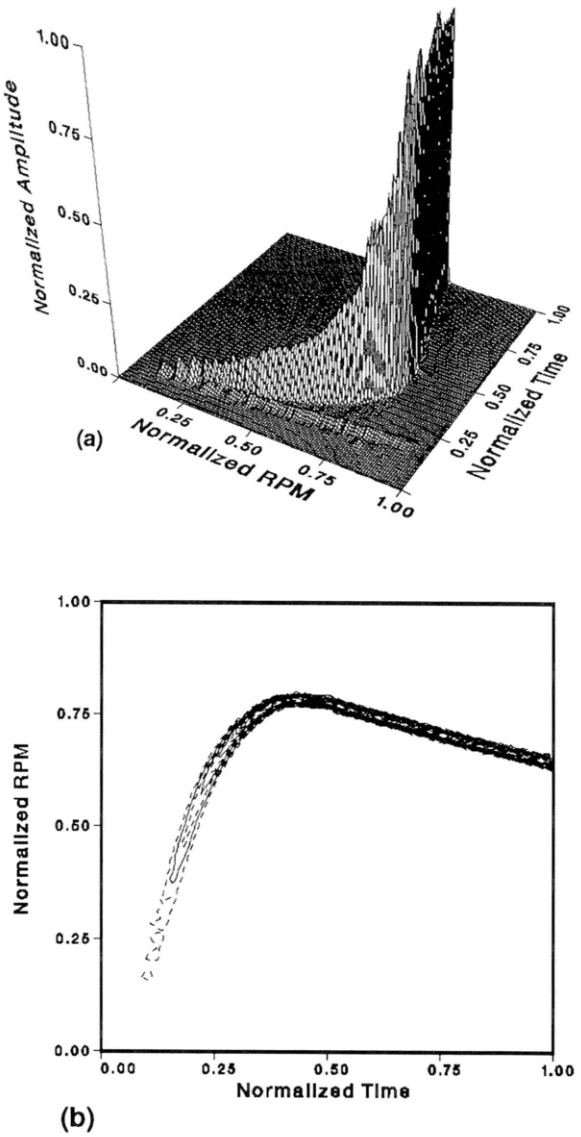

FIGURE 11 Pseudo Wigner–Ville distribution of transient speed of the pump. (a) PWVD and (b) contour plot.

Actual Pump Start-Up RPM Signal

The start-up transient speed of the pump was measured and the results shown in Fig. 11. The PWVD is shown in Fig. 11(a) and the contour view is shown in Fig. 11(b). The contour plot shows that the speed of the pmp runs up when initially started, reaches the maximum rpm, and coasts down gradually. Near the maximum speed during the run up, the sweep rate was rapidly decreased and, as a result, the peak value was rapidly increased. When the sweep rate is close to zero at the normalized time of 0.4, the ampli-

tude attains the maximum value. The PWVD represents the change of the vibration condition in the system with time as shown in Figs. 10 and 11.

CONCLUSIONS

The PWVD was investigated and applied to analyzing nonstationary signals typical of transient machinery signatures and steady-state signals of machinery signatures. The results of this research will be a valuable asset for condition monitoring of transient machinery as well as stationary machinery. The following conclusions can be drawn:

1. The PWVD is ideally suited for portraying nonstationary time signals as well as stationary signals.
2. The use of the modified Hamming window to time signals is effective to reduce the edge effect of discontinuity.
3. The use of the analytic signal in calculating the Wigner distribution eliminates aliasing problems.
4. The Gaussian window function for smoothing the Wigner–Ville distribution is very effective and the presence of cross-terms is significantly reduced.
5. Both the amplitude and the main lobe of the PWVD is significantly affected by the sweep rate. As the absolute sweep rate increases, the amplitude of the PWVD decreases and the main lobe becomes wider.
6. The PWVD characterizes the time–frequency domain distribution of the signal well and may be a useful tool for machinery condition monitoring.

We would like to express our sincere appreciation to Naval Sea Systems Command, PMS390T for their continuing interest in and support of advanced machinery condition monitoring research at Naval Postgraduate School.

REFERENCES

Bartelt, H. O., Brenner, K. H., and Lohmann, A. W., 1980, "The Wigner Distribution Function and Its Optical Production," *Optics Communications,* Vol. 32, pp. 32–38.

Bastiaans, M. J., 1978, "The Wigner Distribution Function Applied to Optical Signals and Systems," *Optics Communications,* Vol. 25, pp. 26–30.

Bastiaans, M. J., 1979, "Wigner Distribution Function and Its Application to First-Order Optics," *Journal of the Optical Society of America,* Vol. 69, pp. 1710–1716.

Cartwright, N. D., 1976, "A Non-Negative Wigner-Type Distribution," *Physica,* Vol. 83A, pp. 210–212.

Claasen, T., and Mecklenbrauker, W., 1980, "The Wigner Distribution—A Tool for Time–Frequency Signal Analysis," *Philips Journal of Research,* Vol. 35, Part I: pp. 217–250, Part II: pp. 276–300, Part III: pp. 372–389.

Cohen, L., 1989, "Time-Frequency Distribution—A Review," *Proceedings of the IEEE,* Vol. 77, pp. 941–981.

Flandrin, P., Garreau, D., and Puyal, C., 1989, "Improving Monitoring of PWR Electrical Power Plants 'In Core' Instrumentation with Time-Frequency Signal Analysis," *IEEE International Conference on Acoustics, Speech, and Signal Processing,* Vol. 4, pp. 2246–2249.

Forrester, B., 1990, "Analysis of Gear Vibration in the Time–Frequency Domain," *Proceedings of the 44th Meeting of the Mechanical Failures Prevention Group,* pp. 225–234.

Jeon, J. J., and Shin, Y. S., 1993, "Pseudo Wigner–Ville Distribution, Computer Program, and its Applications To Time–Frequency Domain Problems," NPS Technical Report NPS-ME-93-002.

Mark, W. D., 1970, "Spectral Analysis of the Convolution and Filtering of Non-Stationary Stochastic Processing," *Journal of Sound and Vibration,* Vol. 11, pp. 19–63.

Otens, R. K., and Enochson, L., 1978, *Applied Time Series Analysis,* Chap. 4, John Wiley & Sons.

Riley, M., 1989, *Speech Time–Frequency Representations,* Kluwer Academic Publishers, New York.

Rossano, G. W., Hamilton, J. F., and Shin, Y. S., "The Pseudo Wigner–Ville Distribution as a Method for Machinery Condition Monitoring of Transient Phenomia," *Proceedings of the 2nd International Machinery Monitoring & Diagnostics Conference,* Los Angeles, CA. October 22–25, 1990, pp. 167–173.

Velez, E., and Absher, R., 1989, "Transient Analysis of Speech Signals Using the Wigner Time–Frequency Representation," *IEEE International Conference on Acoustics, Speech, and Signal Processing,* Vol. 4, pp. 2242–2245.

Ville, J., 1948, "Theorie et Applications de la Notion de Signal Analytique," *Cables et Transmission,* Vol. 2a, pp. 61–74.

Wahl, T., and Bolton, J., 1990, "The Use of the Wigner Distribution to Analyze Structural Impulse Responses," *International Congress on Recent Developments in Air and Structure-Borne Sound.*

Wigner, E., 1932, "On the Quantum Correction for Thermodynamic Equilibrium," *Physics Review,* Vol. 40, pp. 749–759.

Yen, N., 1987, "Time and Frequency Representation of Acoustic Signals by Means of the Wigner Distribution Function: Implementation and Interpretation," *Journal of the Acoustical Society of America,* Vol. 81, pp. 1841–1850.